ORIGINAL PAPER

The role of cathode distribution in gas/liquid/solid multiphase corrosion systems

Jing Jiang · Jia Wang

Abstract Cathode distribution on a metal surface, depending on the total length of three-phase boundary per unit area (L_{tpb}), is an important factor influencing corrosion behavior of metals in gas/liquid/solid multiphase corrosion systems. The effect of L_{tpb} on cathodic oxygen reduction process was first studied by steady-state polarization technique, and the result showed that the cathodic-limiting current densities linearly increased with increasing L_{tpb}, indicating that the cathode distribution had an important influence on the corrosion behavior of metals. On this basis, a model is developed to establish the correlation between the cathodic-limiting current and L_{tpb}. In the model, a general expression for the cathodic-limiting current distribution in TPB zone is deduced, and a linear dependence of the total cathodic-limiting current density on L_{tpb} is established. The simulation result is in good agreement with experimental data.

Keywords Cathode distribution · Three-phase boundary · Gas/liquid/solid multiphase corrosion systems · Cathodic oxygen reduction process · Modeling

Nomenclature

List of symbols

A	Dimensionless constant (6)
a	Dimensionless constant (6)
$C_{O_2,bulk}$	Dissolved oxygen concentration in bulk zone (mmol·L^{-1})
$C_{O_2,tpb}$	Dissolved oxygen concentration in TPB zone (mmol·L^{-1})
D_{O_2}	Diffusion coefficient of oxygen (cm^2·s^{-1})
F	Faraday constant (9.6495×10^4 C·g·mol^{-1})
I_d	Total cathodic diffusion-limiting current (μA) (2)
i_d	Total cathodic diffusion-limiting current density (μA·cm^{-2}) (24)
$I_{d,\,bulk}$	Cathodic diffusion-limiting current of bulk zone (μA)
$i_{d,\,bulk}$	Cathodic diffusion-limiting current density of bulk zone (μA·cm^{-2}) (4)
$I_{d,\,tpb}$	Cathodic diffusion-limiting current of TPB zone (μA) (20)
$\overline{i_{d,tpb}}$	Cathodic diffusion-limiting current density of TPB zone (μA·cm^{-2}) (23)
L	Length of TPB zone (cm)
n	Number of transferred electrons
r	Radius of droplet (cm)
S_{tpb}	Electrode reaction area of TPB zone (cm^2) (22)
S_{bulk}	Electrode reaction area of bulk zone (cm^2) (26)
w	Width of TPB zone (μm) (7)

Greek symbols

φ	Diameter of metal wire (mm)
θ	Contact angle (°)
δ	Thickness of electrolyte layer (μm)

Subscripts

d	Due to the diffusion
tpb	In TPB region
bulk	In bulk region

J. Jiang (✉) · J. Wang
Ocean University of China,
Qingdao 266100, China
e-mail: endeavorgirl1980@yahoo.com.cn

J. Wang
State Key Laboratory for Corrosion and Protection of Metals,
Shenyang 110016, China

Introduction

Study of corrosion behavior of metals in gas/liquid/solid multiphase corrosion systems, such as atmosphere, ocean splash zone, soil and reinforced concrete, has received increasing interest in recent years [1]. Gas/liquid/solid multiphase corrosion system is characterized by dispersion behavior of liquid on metal surfaces. Assuming that liquid exists in the form of droplets, the surface under the droplet functioned as an anode and the surface at the droplet periphery functioned as a cathode [2]. Based on this assumption, highly dispersive liquid leads to the presence of a large amount of dispersive cathodes on a metal surface, which greatly accelerates the corrosion rates of metals. The fact that corrosion rates of structural steels in splash zone was much higher than that under continuous immersion in seawater [3] and a higher corrosion rate was frequently observed at 60–65% water content of their water holding capacity (WHC) in soil than that in water-saturated soil [4], confirmed the acceleration of the corrosion process with the presence of a large amount of dispersive cathodes. Accordingly, cathode distribution on metal surfaces is an important factor influencing corrosion process in gas/liquid/solid multiphase corrosion systems, and study of its role in multiphase corrosion systems on corrosion behavior of metals is of great significance. Yet, until today, little attention has been paid to the related work in this area.

Extensive studies showed that the electrochemical reaction area at droplet periphery, i.e., the area in which the electrolyte layer thickness ranges from 0 to 100 µm, was a high-speed cathodic reaction area, in which the diffusion rate of oxygen was much higher than that in bulk solution [5–7]. Therefore, cathode distribution can be described by the proportion of total surface area at droplet periphery to the total surface area under droplet, which is closely related to total length of three-phase boundary of dispersive liquid on a metal surface. In this paper, a parameter L_{tpb}, representing the TPB length per unit area, is used to evaluate the cathode distribution on a metal surface, which is expressed as

$$L_{tpb} = \frac{2\pi r}{\pi r^2} = \frac{2}{r} \tag{1}$$

where r is the droplet radius. Note that an increase of cathode distribution is caused by an increase of L_{tpb}. Thus the study of effect of TPB length on cathodic and corrosion process of metals can reflect the important role of cathode distribution in gas/liquid/solid multiphase corrosion systems.

The objective of this paper are, first, to clarify the effect of L_{tpb} on cathodic process of metals, second, to evaluate the role of cathode distribution in gas/liquid/solid multi-phase corrosion systems by constructing a model.

Experimental

The effect of L_{tpb} on cathodic process of metals under an electrolyte droplet was studied by steady-state polarization technique in a three-electrode cell (Fig. 1). The specimen prepared from a plate of A3 carbon steel with the exposed area of 50×50 mm^2 was used as working electrode. A saturated calomel electrode (SCE) connected with the electrolyte using a lugging capillary was used as reference electrode, and a Pt wire (0.5 mm φ) was used as counter electrode. Electrolyte with different volume was dropped onto the working area using a micropipette to form droplet with different size. To avoid the evaporation of the droplet, the cell was placed inside a humidity-controlled chamber to keep the humidity at 85% RH. Prior to each experiment, the working area was finally wet-ground with 1,000-grade emery papers, washed in de-ionized water, degreased with alcohol, and then dried with warm air. The electrolyte was 0.1 M NaCl solution, prepared from the analytical grade reagent and de-ionized water.

Steady-state polarization tests were done potentiostatically from E_{corr} to −1.0 V/SCE at an interval of 50 mV by using a potentiostat/galvanostat (PAR273A, America). The current was recorded after polarizing 1 min at each potential, and the droplet was photographed using a digital CCD camera (Pixera, America). From the picture of the droplet, the accurate droplet size was read and the contact angle was determined by measuring the tangent to the droplet at its intersection with the metal surface by using software Adobe Photoshop 7.0.

Results and discussion

Effect of L_{tpb} on cathodic oxygen reduction process of metals under a 0.1 M NaCl droplet

Figure 2 shows the cathodic-limiting current densities taken at −900 mV/SCE on both A3 carbon steel and 304 stainless steel surfaces as a function of L_{tpb}. It was observed that the cathodic-limiting current densities for two sorts of metals
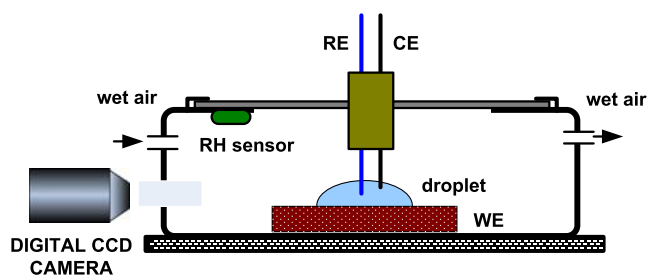

Fig. 1 The schematic diagram of the three-electrode cell for an electrolyte droplet attached on a planar electrode surface

linearly increased with increasing L_{tpb}, indicating the important influence of L_{tpb} on cathodic oxygen reduction process. A simple estimation based on the linear-fitting equation in Fig. 2, reveals that the cathodic-limiting current density has a 0.5-fold increase when L_{tpb} increases twice, confirming the significant role of cathode distribution in gas/liquid/solid multiphase corrosion systems.

Modeling cathodic oxygen reduction process under an electrolyte droplet

Division of electrochemical reaction area under a droplet

The electrochemical reaction area under the droplet can be divided into two parts: one is the surface under droplet periphery in which the electrolyte layer thickness ranges from 0 to $100\,\mu m$, and the other is the surface under the center area of droplet in which the electrolyte layer thickness is greater than $100\,\mu m$. The former is named

"TPB region" and the latter is "bulk region". The schematic diagram is shown in Fig. 3. Accordingly, when the system was under cathodic polarization, the limiting current flows through these two regions, i.e.:

$$I_d = I_{d,bulk} + I_{d,tpb} \tag{2}$$

Let S_{bulk} be the area of bulk region and S_{tpb} the area of TPB region, then

$$I_d = i_{d,bulk} \times S_{bulk} \times i_{d,tpb} \times S_{tpb} \tag{3}$$

where i_{bulk} is the cathodic-limiting current density in bulk region, given by

$$i_{d,bulk} = nFD_{O_2} \frac{C_{O_2,bulk}}{100\mu m} \tag{4}$$

where n is the number of transferred electrons, F is the Faraday constant, D_{O_2} is the diffusion coefficient of oxygen, and $C_{O_2,bulk}$ is the concentration of dissolved oxygen in bulk region. Since $C_{O_2,bulk}$ is only dependent on concentration of electrolyte, i_{bulk} is constant under a certain concentration of electrolyte.

However, in TPB region, the cathodic-limiting current density ($i_{d,tpb}$) depends strongly on the thickness of electrolyte layer. Some studies reveal that [5–7] the cathodic-limiting current of metals under thin electrolyte layer first increases and then decreases with a reduction in δ, and the maximum position is a little shifted in the range of 20–$30\,\mu m$ according to the experiment conditions. Based on the tendency of $i_{d,\ tpb}$–δ mentioned above, the TPB region can be roughly divided into three parts, as shown in Fig. 4. The corresponding cathodic-limiting current density, $i_{d,\ tpb,\ i}$ $(i=1,\ 2,\ 3)$, can be expressed as

I.　$30\,\mu m < \delta < 100\,\mu m$

The cathodic-limiting current density in this part increases with a reduction in δ, given by

$$i_{d,tpb,1} = nFD_{O_2} \frac{C_{O_2,tpb}}{\delta} \tag{5}$$

where n, F, D_{O_2} is the same as in Eq. (4), and $C_{O_2,tpb}$ is the concentration of oxygen in TPB region;
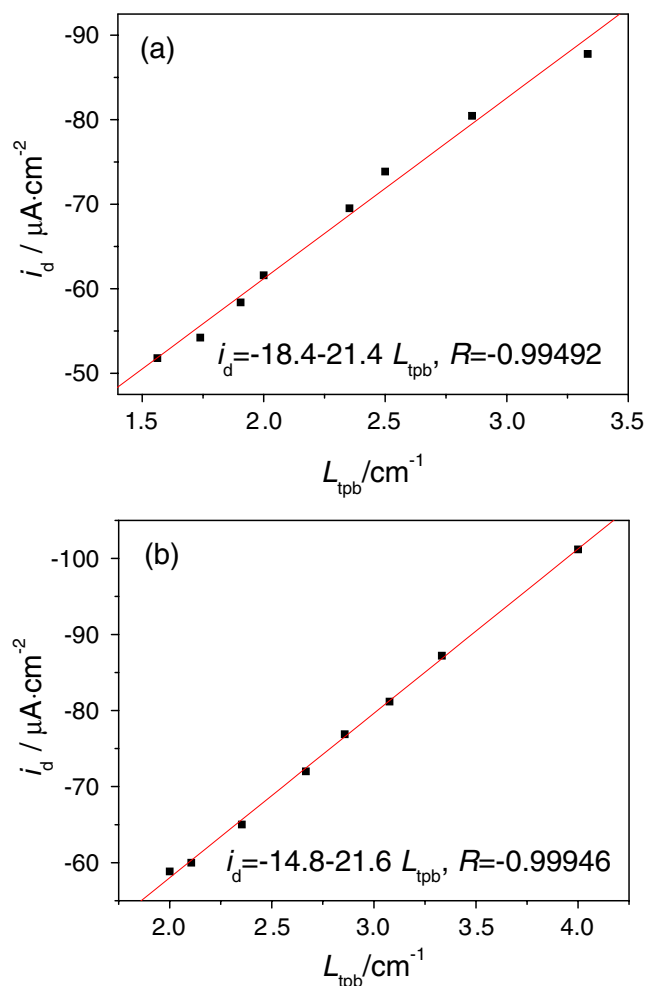

Fig. 2 Cathodic-limiting current densities of metals under a 0.1 M NaCl droplet taken at -900 mV/SCE as a function of L_{tpb}. **a** A3 carbon steel, **b** 304 stainless steel
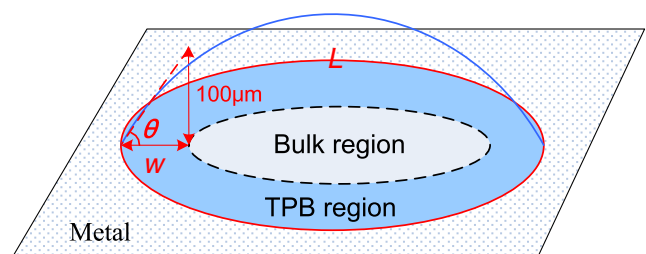
Fig. 3 The geometry of an electrolyte droplet attached on a planar metal surface

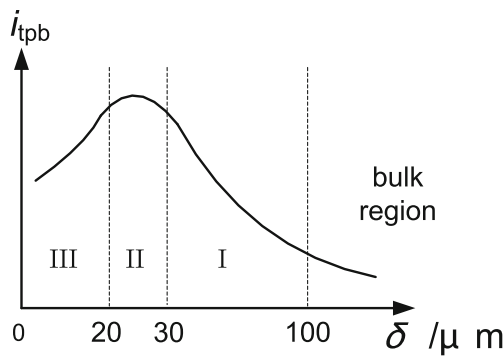**Fig. 4** The schematic diagram of division of the TPB region

II. $20\,\mu m<\delta<30\,\mu m$

$i_{d,\,tpb}-\delta$ curve in this part is approximated as a plateau and $i_{d,\,tpb,\,2}$ is assumed to be constant;

III. $0<\delta<20\,\mu m$

The cathodic-limiting current density in this part rapidly decreases with a reduction in δ. In this case, the interface of metal/electrolyte layer can be represented by a transmission line (TML) circuit in which the current distribution over the electrode surface is considered [8]. Based on the TML model, Eq. (6) is obtained by the analysis of current distribution in this part [7].

$$i_{d,tpb,3} = A \times \delta^{a/2} \qquad (6)$$

where A and a are dimensionless constants.

Formula derivation for cathodic-limiting current in TPB region

Note that the TPB region is in a shape of thin ring which can be approximated as a thin band of length L ($L=2\pi r$) and width w. Here, w can be expressed as (Fig. 3)

$$w = 100\,\mu m \times \cot\theta \qquad (7)$$

where θ is liquid/metal contact angle in relation with the surface quality of metal.

Let axis x (the horizontal line) direct to the liquid internal with the origin at TPB (Fig. 5), then within the zone (x, $x+$
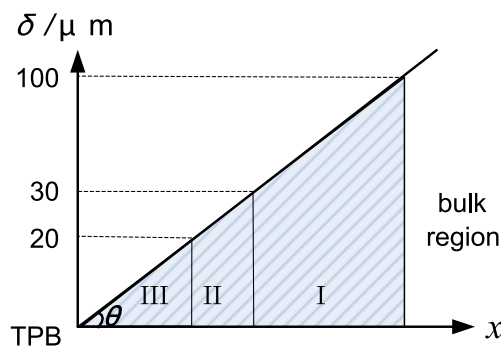

Fig. 5 The schematic diagram of the electrolyte layer thickness as a function of x
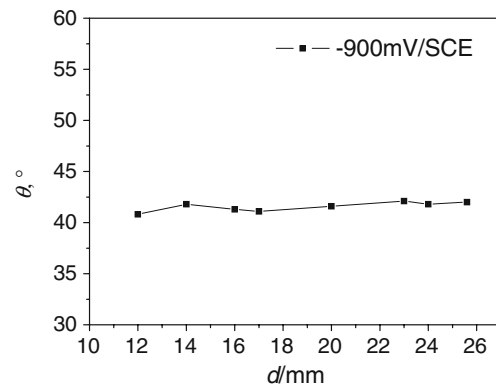

Fig. 6 Contact angle of 0.1 M NaCl droplet attached on A3 carbon steel surface taken at −900 mV/SCE as a function of droplet diameter

dx), the cathodic-limiting current can be given by

$$dI_{d,tpb,i} = i_{d,tpb,i} \times L \times dx \qquad (8)$$

From Fig. 5 we get

$$x = \delta \times \cot\theta \qquad (9)$$

Substituting Eq. (9) into Eq. (8) we get

$$dI_{d,tpb,i} = i_{d,tpb,i} \times L \times d(\delta \cdot \cot\theta) \qquad (10)$$

Note that θ is only potential-dependent [9], independent of the electrolyte thickness and the droplet size (Fig. 6). On this condition, Eq. (10) can be rewritten as

$$dI_{d,tpb,i} = i_{d,tpb,i} \times L \times \cot\theta \times d\delta \qquad (11)$$

Substituting Eqs. (5) and (6) into Eq. (11) and considering $i_{d,\,tpb,2}$ as constant, Eqs. (12)–(14) are obtained

$$dI_{d,tpb,1} = nFD_{O_2} \frac{C_{O_2,tpb}}{\delta} \times L \times \cot\theta \times d\delta \qquad (12)$$

$$dI_{d,tpb,2} = i_{d,tpb,2} \times L \times \cot\theta \times d\delta \qquad (13)$$

$$dI_{d,tpb,3} = A \times \delta^{a/2} \times L \times \cot\theta \times d\delta \qquad (14)$$
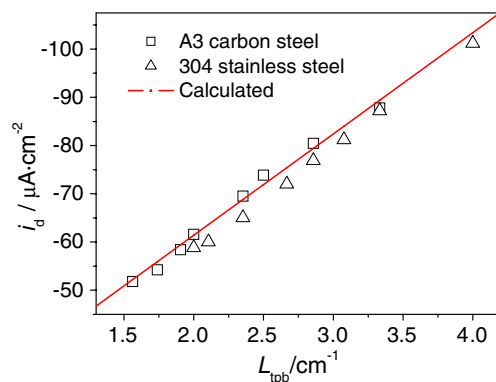

Fig. 7 Comparison between simulation result and experimental data for the L_{tpb} effect on cathodic process of metals

Integrating Eq. (12) from 30 to 100 μm we get

$$I_{d,tpb,1} = nFD_{O_2}C_{O_2,tpb} \times L \times \cot\theta \times \int_{30}^{100} \frac{d\delta}{\delta}$$

$$= \ln\frac{10}{3} nFD_{O_2}C_{O_2,tpb} \times L \times \cot\theta \qquad (15)$$

Integrating Eq. (13) from 20 to 30 μm we get

$$I_{d,tpb,2} = i_{d,tpb,2} \times L \times \cot\theta \times \int_{20}^{30} d\delta$$

$$= 0.001 \times i_{d,tpb,2} \times L \times \cot\theta \qquad (16)$$

Integrating Eq. (14) from 0 to 20 μm we get

$$I_{d,tpb,3} = A \times L \times \cot\theta \int_{0}^{20} \delta^{a/2} d\delta$$

$$= \frac{A \times (0.002)^{1+a/2}}{1+a/2} \times L \times \cot\theta \qquad (17)$$

The total cathodic-limiting current in TPB region flows through above three parts, i.e.:

$$I_{d,tpb} = \sum_i I_{d,tpb,i} = I_{d,tpb,1} + I_{d,tpb,2} + I_{d,tpb,3} \qquad (18)$$

Substituting Eqs. (15)–(17) into Eq. (18) and rearranging we get

$$I_{d,tpb} = \left(\ln\frac{10}{3} nFD_{O_2}C_{O_2,tpb} + 0.001 \cdot i_{d,tpb,2} \right. \qquad (19)$$

$$\left. + \frac{A \times (0.002)^{1+a/2}}{1+a/2} \right) \times L \times \cot\theta$$

Taking into account that both $C_{O_2,tpb}$ and $i_{d,tpb,2}$ are only concentration-dependent [5] and can be considered as constants under a fixed concentration of electrolyte, Eq. (19) can be rewritten as

$$I_{d,tpb} = Const \times L \times \cot\theta \qquad (20)$$

where

$$Const = \ln\frac{10}{3} nFD_{O_2}C_{O_2,tpb} + 0.001 \times i_{d,tpb,2}$$

$$+ \frac{A \times (0.002)^{1+a/2}}{1+a/2} \qquad (21)$$

The electrode reaction area of the TPB region, S_{tpb}, is given as

$$S_{tpb} = L \times w = 100\,\mu m \times L \times \cot\theta \qquad (22)$$

Substitution of Eq. (22) into Eq. (20) leads to

$$\overline{i_{d,tpb}} = \frac{Const}{100\mu m} \qquad (23)$$

Table 1 Model parameter values

Parameter	Value
n	4
F	$9.6495 \times 10^4\,C \cdot g \cdot mol^{-1}$
D	$1.9 \times 10^{-5}\,cm^2 \cdot s^{-1}$
$C_{O_2,bulk}$	0.1 mmol·L^{-1}
$C_{O_2,tpb}$	0.18 mmol·L^{-1}
$i_{d,\,tpb,\,2}$	1 mA·cm^{-2} [5–7]
A	0.624 [7]
a	1.9 [7]
$i_{d,\,bulk}$	73 μA·cm^{-2}
$\overline{i_{d,tpb}}$	245 μA·cm^{-2}
θ (-900 mV/SCE)	40°

From Eq. (23) we can see that $\overline{i_{d,tpb}}$ is constant under a fixed concentration of electrolyte.

Modeling effect of L_{tpb} on cathodic-limiting current density under a droplet

Dividing both sides of Eq. (3) by the area of droplet, πr^2, we get

$$i_d = i_{d,bulk} \cdot \frac{S_{bulk}}{\pi r^2} + \overline{i_{d,tpb}} \cdot \frac{S_{tpb}}{\pi r^2} \qquad (24)$$

It is known that,

$$\pi r^2 = S_{bulk} + S_{tpb} \qquad (25)$$

Substituting Eq. (22) into Eq. (25) and rearranging we get

$$S_{bulk} = \pi r^2 - 2\pi r \cdot 100\mu m \cdot \cot\theta \qquad (26)$$

Substituting Eqs. (22) and (26) into Eq. (24) and rearranging we get

$$i_d = i_{d,bulk} + (\overline{i_{d,tpb}} - i_{d,bulk}) \cdot 100\,\mu m \times \frac{2}{r} \times \cot\theta \qquad (27)$$

Based on Eq. (1), Eq. (27) can be rewritten as

$$i_d = i_{d,bulk} + (\overline{i_{d,tpb}} - i_{d,bulk}) \times 100\,\mu m \times \cot\theta \times L_{tpb} \qquad (28)$$

From Eq. (28), we can see that since θ, $i_{d,\,bulk}$ and $\overline{i_{d,tpb}}$ are constant under a certain polarization potential and electrolyte concentration, the cathodic-limiting current density of metals under the droplet (i_d) linearly depends on TPB length per unit area (L_{tpb}). Taking into account that $\overline{i_{d,tpb}} >> i_{d,bulk}$, a linear increase of i_d with increasing L_{tpb} is concluded based on Eq. (28), in accordance with the experimental data in Fig. 2.

Model validation

The parameter values are listed in Table 1.

The i_d as a function of L_{tpb} is calculated using Eq. (28) with the parameter values in Table 1. The comparison of the calculated result and experimental data is shown in Fig. 7. The simulation result is in good agreement with the experimental data.

Conclusion

Cathode distribution on a metal surface, depending strongly on the length of three-phase boundary per unit area, is an important factor influencing corrosion process in corrosion systems with highly dispersive liquid. The parameter L_{tpb} is used to evaluate the cathode distribution in this paper.

The effect of L_{tpb} on the cathodic process of metals under an electrolyte droplet was studied by steady-state polarization technique. The results showed that cathodic-limiting current densities linearly increased with increasing L_{tpb}, confirming the important role of cathode distribution in gas/liquid/solid multiphase corrosion systems. In addition, the effect of cathode distribution on cathodic oxygen reduction process of metals was simulated. The simulation result showed a linear increase of i_d with increasing L_{tpb}, in good agreement with the experimental data.

One may expect that this work is of great significance for clarifying the corrosion mechanism as well as predicting corrosion process in gas/liquid/solid multiphase corrosion systems.

Reference

1. Chu-nan C (2005) Nature environment corrosion of materials in China. Chemical Industry, Beijing
2. Cai JP, Lyon SB (2005) Corros Sci 47:2956. doi:10.1016/j.corsci.2005.04.011
3. Nunez L, Reguera E, Corvo F, Gonzalez E, Vazquez C (2005) Corros Sci 47:461. doi:10.1016/j.corsci.2004.05.015
4. Gupta SK, Gupta BK (1979) Corros Sci 19:171. doi:10.1016/0010-938X(79) 90015-5
5. Tsuru T, Nishikata A, Jia W (1995) Mater Sci Eng 198:161. doi:10.1016/0921-5093(95) 80071-2
6. Nishikata A, Ichihara V, Hayashi V, Tsuru T (1997) J Electrochem Soc 144:1244. doi:10.1149/1.1837578
7. Jia W, Tsuru T (1995) J Chin Soc Corros Protec 15:180
8. Nishikata A, Ichihara Y, Tsuru T (1995) Corros Sci 37:897. doi:10.1016/0010-938X(95) 00002-2
9. Jin-Hua C, Shi-Hui S, Li-Hua N, Shou-Zhuo Y (1997) Electrochim Acta 42:689. doi:10.1016/S0013-4686(96) 00230-7